

## **ELECTRON MICROSCOPY STUDY OF MICROSTRUCTURE OF THE OXIDE-DISPERSION-STRENGTHED STEEL**

**H. Xing<sup>1</sup>, J. Sun<sup>1\*</sup>, Z. J. Zhou<sup>2</sup>**

<sup>1</sup> Electron Microscopy Laboratory, School of Materials Science and Engineering,  
Shanghai Jiaotong University, Shanghai 200240, P. R. China

<sup>2</sup> School of Materials Science and Engineering,  
University of Science and Technology Beijing, Beijing 100083, China

### **Abstract**

The microstructure of the ODS ferritic-martensitic steel with chemical composition of Fe-12Cr-2W-0.5Ti-0.2V-0.2Si-0.13C-0.35Y<sub>2</sub>O<sub>3</sub> wt% fabricated by MA and HIP has been investigated by TEM. The emphasis is focused on the structure and chemical composition of the fine ODS particles and inclusions. The results showed that two types of complex ODS particles such as Y-Ti-O and Y-Si-O with nanometer size distribute homogeneously and incoherently in the matrix of the steel. Additionally, large (Ti,V)N inclusions were observed in the steel. The results of microstructural characterization are discussed to correlate with the processing and mechanical properties of the ODS steel.

### **1. Introduction**

Oxide-dispersion-strengthened (ODS) ferritic-martensitic steels produced by mechanical alloying (MA) and hot isostatic pressing (HIP) techniques have excellent thermal properties, higher swelling resistance and outstanding creep resistance, which are superior to these of austenitic steels [1, 2]. Thus, they have attracted growing interest as candidate cladding material for supercritical-water cooled reactors (SCWR). In the past few years, pure Y<sub>2</sub>O<sub>3</sub> and Y<sub>2</sub>O<sub>3</sub> with Al or Ti were generally chosen as the constituents of the ODS particles [3-6]. The additional elements lead to the formation of complex ODS particles and other nanosized impurities with different morphologies, chemical compositions and spatial distributions, which are of major influence on the mechanical properties of the steels. Therefore, knowledge of the microstructure, particularly the nano-features of the various particles is necessary in order to improve the understanding of the relationship between the microstructure and mechanical properties of the ODS ferritic-martensitic steels.

In this paper, a systematical transmission electron microscopy (TEM) study on the complex ODS particles and other inclusions in the ODS ferritic-martensitic steel with chemical composition of Fe-12Cr-2W-0.5Ti-0.2V-0.2Si-0.13C-0.35Y<sub>2</sub>O<sub>3</sub> wt% is presented. Energy dispersive X-ray (EDX) and electron-energy loss spectroscopy (EELS) analyses were conducted to obtain information on the chemical composition and electronic structure of the complex ODS particles

and other inclusions in this ODS ferritic-martensitic steel. Some implications of the results of this microstructural characterization are discussed to correlate with the processing and mechanical properties of the ODS ferritic-martensitic steel.

## 2. Materials and methods

The ODS ferritic-martensitic steel was produced by mechanical alloying of pulverized alloy powders with a chemical composition of Fe-12Cr-2W-0.5Ti-0.2V-0.2Si-0.13C wt% ( $\sim 75\ \mu\text{m}$  size) together with 0.35 wt%  $\text{Y}_2\text{O}_3$  powders ( $\sim 30\ \text{nm}$  diameter) in a high-energy planetary ball mill. Argon gas was used as an inert atmosphere during MA to keep the oxygen and nitrogen content as low as possible. Repeated impacts of energetic balls during MA resulted in a fairly homogeneous distribution of nanosized  $\text{Y}_2\text{O}_3$  particles in the steel matrix. Then, the MA steel powders were degassed at  $450^\circ\text{C}$  in vacuum and sealed in a stainless steel container. The canister was consolidated by hot isostatic pressing (HIP) at  $1150^\circ\text{C}$  for 3 hours under a pressure of 70 MPa. The thin foils for TEM observations were prepared by twin jet electro-polishing in a 6 vol% perchloric acid + 94 vol% ethanol solution chilled to about  $-30^\circ\text{C}$  at 30 V. The TEM observations were carried out using a JEM-2100F microscope equipped with an EDX and EELS spectrometer operating at 200 kV. The energy resolution for the EELS analyses is around 0.95 eV at full width at half maximum of the zero-loss peak.

## 3. Results and discussion

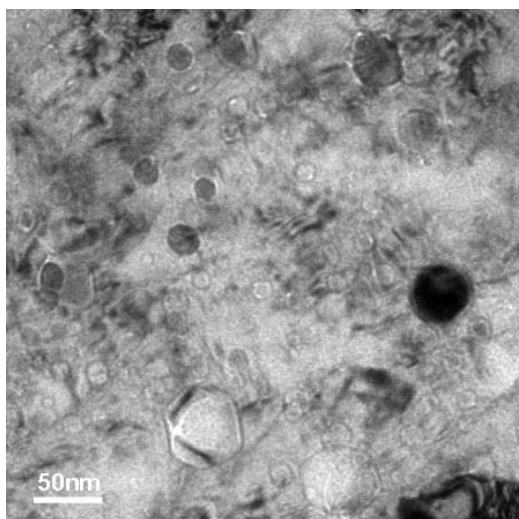


Figure 1 Bright field TEM micrograph of the microstructure of the ODS ferritic-martensitic steel, showing nanosized ODS particles distributed homogeneously in the matrix of the ODS steel.

A typical bright-field TEM micrograph of the microstructure of the ODS ferritic-martensitic steel produced by MA and HIP is shown in Fig. 1. One can see that the nanosized (10~50 nm) ODS

particles distribute homogeneously and incoherently in the matrix of the steel. The ODS particles often have a contrast similar to the surrounding matrix on the TEM micrographs, and are visible as disks decorated at their perimeter. This decoration originates from the Fresnel fringes at boundaries between two phases under the under-focus condition. Sometimes, the ODS particles show different contrast due to their different crystallographic orientations with the matrix of the steel.

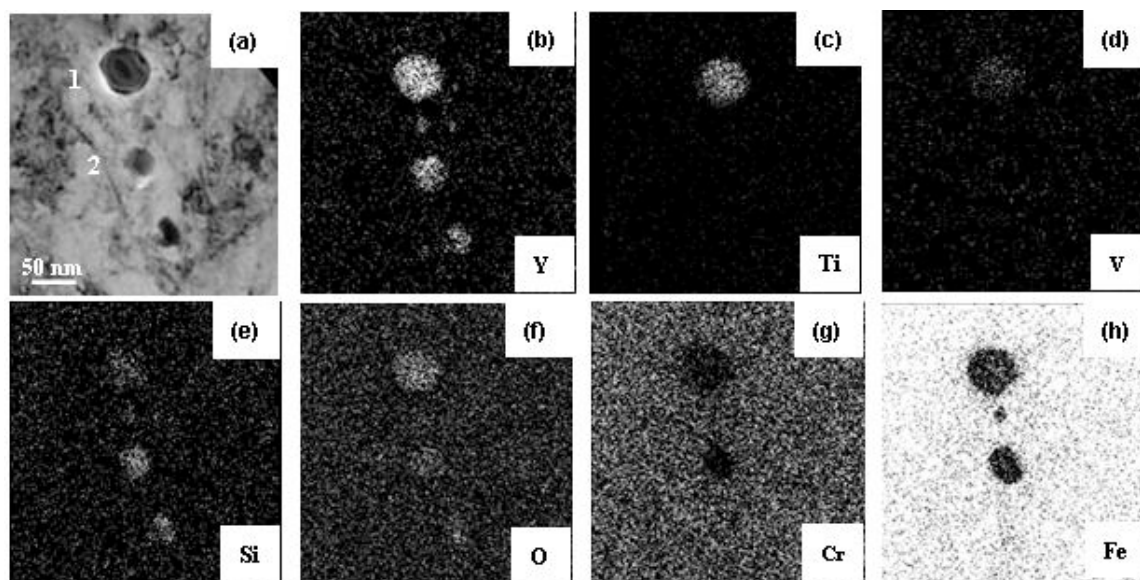


Figure 2 EDX elemental mapping of the complex ODS particles, (a) TEM micrograph, (b)–(h) EDX elemental mapping of Y, Ti, V, Si, O, Cr and Fe, respectively.

The chemical composition of the ODS particles in the ferritic-martensitic steel was further analyzed using the EDX spectrometer attached to the TEM. It was found that there exist two types of complex ODS particles, Y-Si-O and Y-Ti-O oxides, with similar morphologies in the ODS steel. The typical atomic ratio of the Y-Si-O complex oxides was found to be 0.31: 0.25: 1, corresponding a chemical composition of  $Y_{2.16}Si_{1.76}O_7$ . The typical chemical composition of the Y-Ti-O complex oxides was found to be  $Y_{2.15}Ti_{1.95}O_7$  with small amount of Si and V (less than 1.3 at.%). This is consistent with earlier results reported by Klimiankou *et al.* and Okuda *et al.* respectively [7, 8]. Figure 2 shows a bright field TEM micrograph and EDX elemental mapping of several ODS particles in the steel. It can be seen that the particle marked '1' is rich in Y, Ti and O and shows slight segregation of V and Si. On the other hand, the particle marked '2' is rich in Y, Si and O. These observations clearly reveal the formation of the two types of complex ODS particles; Y-Ti-O and Y-Si-O. The EDX spectra acquired from the numerous ODS dispersoids with different sizes do not provide any evidence of the presence of pure  $Y_2O_3$  in the steel.

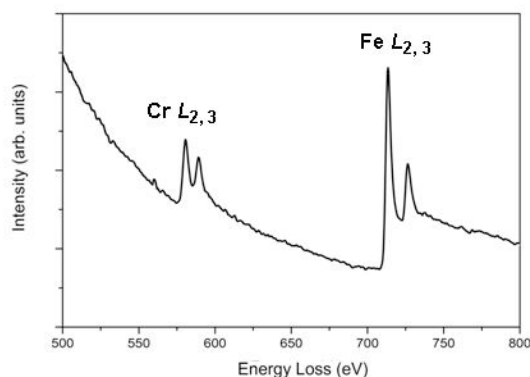


Figure 3 The EELS spectrum acquired from the matrix.

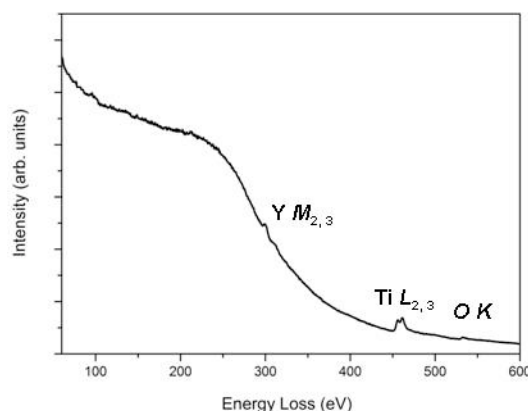


Figure 4 EELS spectrum taken from the Y-Ti-O complex ODS particles.

The EELS spectra obtained from the embedded ODS particles not only give chemical composition but also reflect the electronic structure of the unoccupied states of the complex oxides in the ODS steel. In particular, the O- $K$  edge is very distinctive of the electronic structure of the complex oxides. Figure 3 shows the EELS spectrum acquired from the matrix, and only Fe- $L_{2,3}$  and Cr- $L_{2,3}$  edges are observed in this spectrum, reflecting contributions mainly from the matrix of the steel. The EELS spectrum taken from an Y-Ti-O complex ODS particle is shown in Figure 4. The observed EELS features were identified as the Ti- $L_{2,3}$ , O- $K$ , and Y- $M_{2,3}$  edges, which is consistent with the EDX results. Figure 5 shows O  $K$  and Ti  $L_{2,3}$  edge fine structures acquired from the Y-Ti-O complex ODS particles. The two spectra, are presented after background subtraction. One can see that there are three pronounced peaks, marked as  $a_1$ ,  $a_2$ , and  $a_3$ , in the O  $K$  edge fine structure, which is similar to spectra reported in Reference 7, although the maximum position of the spectrum is somewhat different. In contrast, only two peaks appear in the O  $K$ -edge structure from the pure  $Y_2O_3$  oxides. The two peaks were considered to be the

signature of the tetrahedral arrangement of oxygen atoms in  $Y_2O_3$  and reflect the density of O 2p states hybridized with Y 4d orbitals on formation of the  $Y_2O_3$  conduction band [9, 10]. Correspondingly, the Ti  $L_2$  and Ti  $L_3$  lines split up into two peaks, marked as  $b_1$ ,  $b_2$  and  $c_1$ ,  $c_2$ , with an energy separation of 2.15 eV between them.

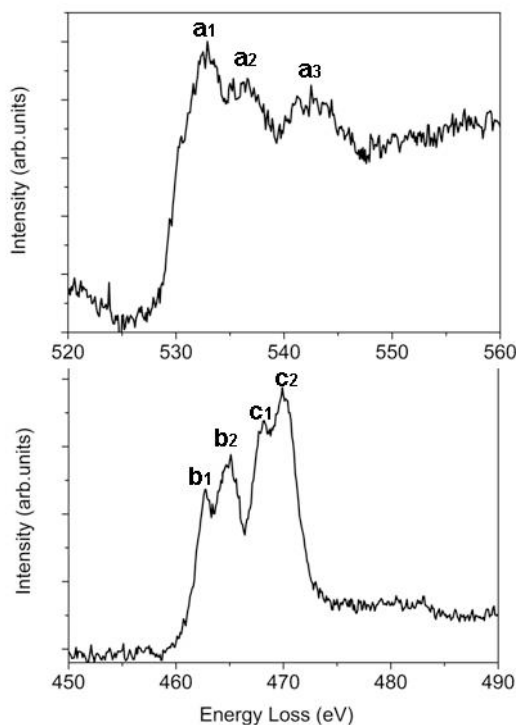


Figure 5 O K edge (a) and Ti  $L_{2,3}$  edge (b) fine structures taken from Y-Ti-O complex ODS particles.

The splitting of the O  $K$  and Ti  $L_{2,3}$  edges can be attributed to the ligand field induced by the six oxygen atoms surrounding the Ti atoms in octahedral symmetry, and the two peaks in the Ti  $L_2$  and  $L_3$  edges are referred to as  $t_{2g}$  and  $e_g$  due to the orbital symmetry. These Y-Ti-O and Y-Si-O complex ODS particles are thought to arise from the chemical reaction between Ti or Si in the alloy powders,  $Y_2O_3$  powders and oxygen in the atmosphere during MA and HIP processes. TEM observations revealed that the nanosized fine complex ODS particles distribute homogeneously and incoherently in the matrix of the steel. Although the Fe-12Cr-2W-0.5Ti-0.2V-0.2Si-0.13C-0.35 $Y_2O_3$  wt% ferritic-martensitic steel was intended to have 0.35 wt%  $Y_2O_3$  ODS particles, the formation of Y-Ti-O and Y-Si-O complex oxides raises the volume fraction of ODS particles in the steel and thus influences the mechanical properties of the steel. Moreover, the thermal stability of these Y-Ti-O and Y-Si-O complex oxides need to be investigated in detail.

In addition to the complex ODS particles, inclusions containing Ti were also observed by TEM in the ODS steel. In general, larger inclusions may degrade the mechanical properties of the steels. Therefore, characterization of these inclusions would not only help to improve the prediction of mechanical properties, but also give some indication as to when they were produced during steel fabrication. Larger inclusions of polygonal form with sizes up to  $\sim 500$  nm often appear brighter than the surrounding matrix on the bright field micrographs. An example of such inclusions is presented in Figure 6(a). Figures 6(b)–(f) show the EDX elemental mapping of Ti, V, N, Cr and Fe, respectively in the inclusion. Ti, Cr and N EDX elemental mapping reflect the presence of (Ti,V)N inclusions in the matrix of the ODS steel. These inclusions are also confirmed by EELS investigations as shown in Figure 7. The N-K, Ti- $L_{2,3}$  and V- $L_{2,3}$  edges are clearly visible in the spectrum acquired from the inclusion. The Ti- $L_{2,3}$  edge fine structure is presented in Figure 8. One can see that there is no peak splitting visible in the Ti  $L_2$  and  $L_3$  edges, which implies that (Ti,V)N is of different electronic structure compared with Y-Ti-O complex ODS particles. Earlier investigations also reported the formation of large Ti(C,N) inclusions in the ODS steel [5]. However, no carbon in the inclusions was detected either using EDX or EELS. These (Ti,V)N inclusions are considered to come from the reaction between Ti and V in the alloy powders and nitrogen in the atmosphere during MA process. Therefore, the nitrogen concentration should be reduced to as low a value as possible in the atmosphere during the MA process in order to eliminate the large Ti-containing inclusions in the ODS steel.

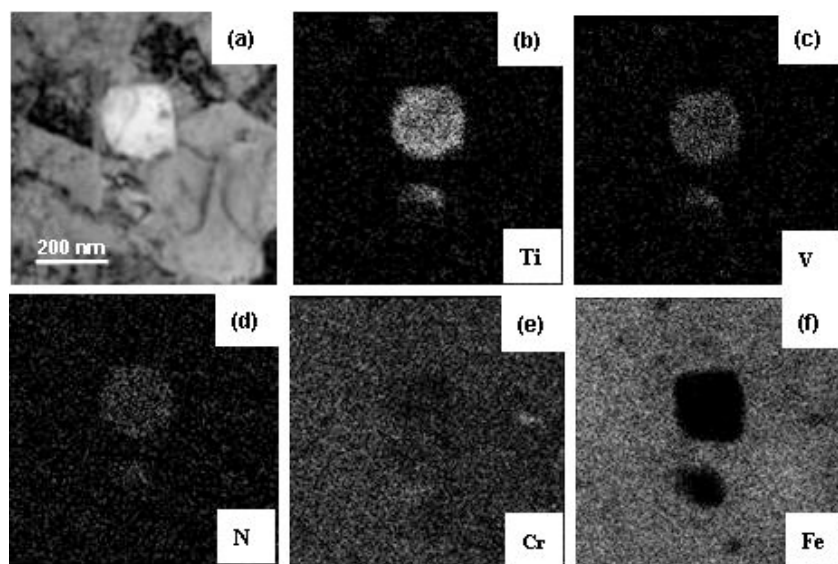


Figure 6 EDX elemental mapping of the inclusions, (a) bright field TEM micrograph, and (b)–(h) EDX elemental mapping of Ti, V, N, Cr and Fe, respectively.

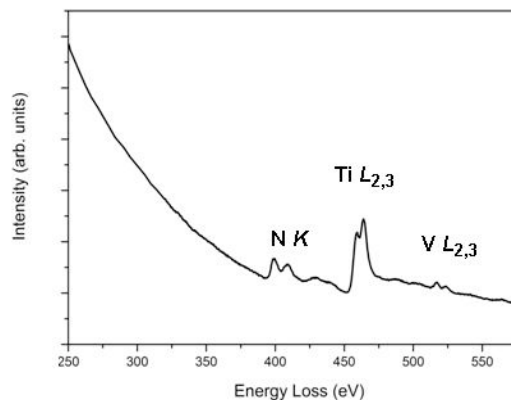


Figure 7 EELS spectrum taken from the (Ti,V)N inclusion.

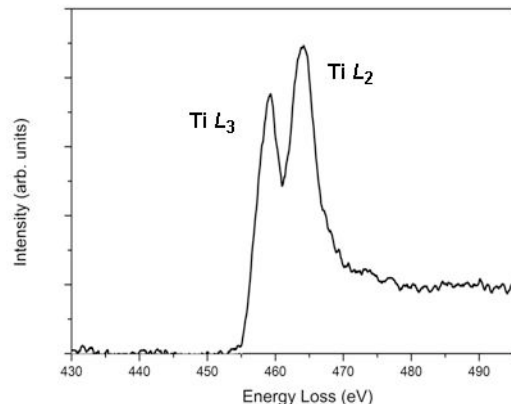


Figure 8 The Ti  $L_{2,3}$  edges fine structure acquired from the (Ti,V)N inclusion.

#### 4. Conclusion

TEM observations show that ODS particles with dimensions of 10~50 nm distribute homogeneously and incoherently in the matrix of the ferritic-martensitic steel with chemical composition of Fe-12Cr-2W-0.5Ti-0.2V-0.2Si-0.13C-0.35Y<sub>2</sub>O<sub>3</sub> wt% fabricated by mechanical alloying and hot isotropic pressing. Two types of Y-Ti-O and Y-Si-O complex ODS particles were found in the steel and were characterized in detail using EDX and EELS in TEM. Apart from the ODS particles, large (Ti,V)N inclusions were observed in the steel. These different ODS particles and inclusions are considered to originate from complex chemical reactions occurring during the MA and HIP processes, and can influence the mechanical properties of the ODS ferritic-martensitic steel.

#### Acknowledgements

This work is supported financially by the National Basic Research Program of China (Project number 2007CB209803).

## References

- [1] M. Klimiankou, R. Lindau, and A. Moslang, "HRTEM study of yttrium oxide particles in ODS steels for fusion reactor application", *Journal of Crystal Growth*, Vol. 249, 2003, pp. 381-387.
- [2] G.R. Odette, M.J. Alinger, and B.D. Wirth, "Recent developments in irradiation-resistant steels", *Annu. Rev. Mater. Res.*, Vol. 38, 2008, pp. 471-503.
- [3] R. Lindau, A. Moslang, M. Schirra, P. Schlossmacher, and M. Klimenkov, "Mechanical and microstructural properties of a hippped RAFM ODS-steel", *Journal of Nuclear Materials*, Vol. 307-311, 2002, pp. 769-772.
- [4] V. de Castro, T. Leguey, A. Munz, M.A. Monge, R. Pareja, E.A. Marquis, S. Lozano-Perez and M.L. Jenkins, "Microstructural characterization of Y<sub>2</sub>O<sub>3</sub> ODS-Fe-Cr model alloys", *Journal of Nuclear Materials*, Vol. 386-388, 2009, pp. 449-452.
- [5] M. Klimiankou, R. Lindau, and A. Moslang and J. Schroder, "TEM study of PM 2000 steel", *Powder Metallurgy*, Vol. 48, No. 3, 2005, pp. 277-287.
- [6] Ch.Ch. Eiselt, M. Klimenkov, R. Lindau, A. Moslang, H.R.Z. Sandim, A.F. Padilha, and D. Raabe, "High-resolution transmission electron microscopy and electron backscatter diffraction in nanoscaled ferritic and ferritic-martensitic oxide dispersion strengthened-steels", *Journal of Nuclear Materials*, Vol. 385, 2009, pp. 231-235.
- [7] M. Klimiankou, R. Lindau, and A. Moslang, "Energy-filtered TEM imaging and EELS study of ODS particles and argon-filled cavities in ferritic-martensitic steels", *Micron*, Vol. 36, 2005, 1-8.
- [8] T. Okuda and M. Fujiwara, "Dispersion behaviour of oxide particles in mechanically alloyed ODS steel", *Journal of Materials Science Letters*, Vol. 14, pp. 1600-1603.
- [9] F. Pailloux, D. Imhoff, M. Jublot, F. Paumier, R.J. Gaboriaud, and M. Jaouen, "HRTEM and EELS study of Y<sub>2</sub>O<sub>3</sub>/MgO thin films", *Micron*, Vol. 37, 2006, pp. 420-425.
- [10] A. Travlos, N. Boukos, G. Apostolopoulos, A. Dimoulas, and C. Giannakopoulos, "EELS study of oxygen superstructure in epitaxial Y<sub>2</sub>O<sub>3</sub> layers", *Materials Science and Engineering B*, 109, 2004, pp. 52-55.